Finite Element Solutions of the Euler Equations for Transonic External Flows

G. S. Baruzzi* and W. G. Habashi†
Concordia University, Montreal, Quebec, H3G 1M8 Canada
and
M. M. Hafez‡
University of California, Davis, Davis, California 95616

This paper presents a finite element Newton-Galerkin scheme for the solution of the steady subsonic and transonic Euler equations, in primitive variable form. The scheme is based on the explicit introduction of an artificial viscosity in the governing equations to provide the necessary dissipation for numerical stability. The system of equations is linearized by a Newton method and a direct solver is used for the resulting fully coupled system of algebraic equations. Convergence of the method is demonstrated to be robust and quadratic, taking very few iterations to reach machine accuracy. Solutions for two-dimensional transonic flows over airfoils are presented including the cases for inviscid subsonic flow around circular cylinders and ellipses.

Nomenclature

A = domain area
DOF = total degrees of freedom of problem
e = element index
E = total number of elements
H = enthalpy
k = element influence matrix
K = global influence matrix
L_2 = residual norm = Σ (R^2)
n = outward normal to domain boundary
N = finite element shape function
p = pressure
q = velocity vector
R = residual of a differential equation
s = distance along domain boundary
u,v = velocity components
U = general variable
$\hat{U}$ = cell-vertex value of variable U
W = Galerkin weight function = N
x,y = Cartesian coordinates
Δ = change in a variable between iterations
γ = isentropic exponent
ν_1,ν_2 = artificial viscosity coefficients
μ = artificial viscosity control parameter
ρ = density
ξ,η = element local coordinate system

Subscripts
i,j = nodal indices
u = contribution from the x-momentum equation
v = contribution from the y-momentum equation
ρ = contribution from the continuity equation
∞ = freestream value

Superscripts
n = iteration number
u = contribution to the u-velocity influence matrix
v = contribution to the v-velocity influence matrix
ρ = contribution to the density influence matrix

I. Introduction

A NUMBER of finite element schemes for the solution of the Euler equations have recently appeared. Fletcher[1] proposed a novel least-squares weighted residual approach for subsonic flows in which each group of primitive variables is discretized, instead of each variable separately. Tezduyar and Hughes[2] have developed Petrov-Galerkin schemes to introduce the necessary artificial viscosity through upwinding operators.

Angrand et al.[3] and Stoufflet[4] have proposed schemes in which integration of the flux terms is performed approximately by mass-lumping operators. The works of Donea,[5] Löhner et al.,[6] and Peraire et al.[7] are based on explicit time marching algorithms, in direct emulation of Lax-Wendroff finite difference schemes. Such explicit methods have slow convergence properties due to the limitations imposed on the time step by the CFL condition. Acceleration techniques such as mass-lumping, local time stepping, multigrid and residual averaging can be introduced to increase the convergence rate. Bruneau et al.[8] have recently proposed, for subsonic and supersonic vortical flows, a finite element scheme based on a least-squares formulation of the steady Euler equations, free of artificial viscosity. The scheme has not, however, been extended to situations with shocks.

The present paper proposes a finite element method where many of the problems and complexities of the previous schemes are avoided. The artificial viscosity needed for the stability of the Galerkin approximation is intentionally chosen to be simple and is the Laplacian of the solution variables, ρ, u, and v, added to the continuity and momentum equations, respectively.[9,10] All three Laplacians are controlled by a single coefficient, uniform throughout the domain, whose value is the minimum one to prevent solution oscillations. The reason for the choice of the simple artificial viscosity form is to avoid possible spurious nonunique solutions of the discrete equations associated with more complicated artificial viscosity forms. In fact, the current trend in solving the Euler equations, using nonlinear artificial viscosity terms with limiters, may lead to illegitimate solutions not related to the solution of the differential equations.[11] It also may lead to slow convergence, limit cycle, or even divergence.[11]

Presented as Paper 90-0405 at the AIAA 28th Aerospace Sciences Meeting, Reno, NV, Jan. 8-11, 1990; received Jan. 25, 1990; revision received July 23, 1990; accepted for publication Aug. 13, 1990.

*Research Associate, Department of Mechanical Engineering, 1455 de Maisonneuve Boulevard West.
†Professor, Department of Mechanical Engineering, 1455 de Maisonneuve Boulevard West.
‡Professor, Department of Mechanical Engineering.

The nonlinear system of equations is linearized by a Newton method that results in quadratic convergence of the iterative process. At each iteration a direct solver is used to solve for the velocities and density in a fully coupled manner. The iterative scheme also permits the recovery of both physically stable and unstable solutions of the Euler system of equations, in multiple solution cases.[12]

II. Theoretical Formulation

Governing Equations

The two-dimensional steady Euler equations are expressed in terms of continuity, momentum, and energy. They can be written in strong conservation form:

$$\frac{\partial(\rho u)}{\partial x}+\frac{\partial(\rho v)}{\partial y}=0 \tag{1a}$$

$$\frac{\partial(\rho u^2+p)}{\partial x}+\frac{\partial(\rho u v)}{\partial y}=0 \tag{1b}$$

$$\frac{\partial(\rho u v)}{\partial x}+\frac{\partial(\rho v^2+p)}{\partial y}=0 \tag{1c}$$

$$p=\frac{\gamma-1}{\gamma}\rho\left(H_\infty-\frac{u^2+v^2}{2}\right) \tag{1d}$$

The simplified energy equation (1d) assumes constant total enthalpy everywhere; a valid assumption for steady flow with no heat transfer at the walls. This, however, does not cause a loss of generality of the formulation, and the approach proposed in this paper is equally valid for the case including the full energy conservation equation.

For stability, an artificial viscosity in the form of Laplacians of the dependent variables is added to each of the governing equations. The nondimensional form of the equations becomes

$$\frac{\partial(\rho u)}{\partial x}+\frac{\partial(\rho v)}{\partial y}=\nu_1\left(\frac{\partial^2\rho}{\partial x^2}+\frac{\partial^2\rho}{\partial y^2}\right) \tag{2a}$$

$$\frac{\partial(\rho u^2+p)}{\partial x}+\frac{\partial(\rho u v)}{\partial y}=\nu_2\left(\frac{\partial^2 u}{\partial x^2}+\frac{\partial^2 u}{\partial y^2}\right) \tag{2b}$$

$$\frac{\partial(\rho u v)}{\partial x}+\frac{\partial(\rho v^2+p)}{\partial y}=\nu_2\left(\frac{\partial^2 v}{\partial x^2}+\frac{\partial^2 v}{\partial y^2}\right) \tag{2c}$$

$$p=\frac{\gamma-1}{\gamma}\rho\left(H_\infty-\frac{u^2+v^2}{2}\right) \tag{2d}$$

where the artificial viscosity coefficients ν_1, ν_2 are functions of a single parameter μ

$$\nu_1=\frac{\mu}{U_\infty L}\qquad \nu_2=\frac{\mu}{\rho_\infty U_\infty L}$$

The pressure can also be eliminated using the energy equation and, in that case, the first term of Eq. (2b) becomes

$$\rho u^2+p=\rho u^2+\frac{\gamma-1}{\gamma}\rho\left(H_\infty-\frac{u^2+v^2}{2}\right)$$

$$=\frac{\gamma+1}{2\gamma}\rho u^2-\frac{\gamma-1}{2\gamma}\rho v^2+\frac{\gamma-1}{\gamma}\rho H_\infty$$

With the pressure eliminated as a variable, the number of equations is reduced to three, from the original four.

Weak-Galerkin Weighted Residual Method

The weighted residual method consists of minimizing the residuals of the system of equations over the solution domain. It is applied to the reduced system of equations as follows:

$$\iint_A W_i\left[\frac{\partial(\rho u)}{\partial x}+\frac{\partial(\rho v)}{\partial y}-\nu_1\left(\frac{\partial^2\rho}{\partial x^2}+\frac{\partial^2\rho}{\partial y^2}\right)\right]dA=0 \tag{3a}$$

$$\iint_A W_i\left[\frac{\partial(\rho u^2+p)}{\partial x}+\frac{\partial(\rho u v)}{\partial y}-\nu_2\left(\frac{\partial^2 u}{\partial x^2}+\frac{\partial^2 u}{\partial y^2}\right)\right]dA=0 \tag{3b}$$

$$\iint_A W_i\left[\frac{\partial(\rho u v)}{\partial x}+\frac{\partial(\rho v^2+p)}{\partial y}-\nu_2\left(\frac{\partial^2 v}{\partial x^2}+\frac{\partial^2 v}{\partial y^2}\right)\right]dA=0 \tag{3c}$$

where W_i is the Galerkin weight function, selected identical to the shape function that describes the behavior of the variable in the element.

The weak form of the equations is obtained by integrating all terms by parts

$$\iint_A\left[\rho u\frac{\partial W_i}{\partial x}+\rho v\frac{\partial W_i}{\partial y}-\nu_1\left(\frac{\partial\rho}{\partial x}\frac{\partial W_i}{\partial x}+\frac{\partial\rho}{\partial y}\frac{\partial W_i}{\partial y}\right)\right]dA$$
$$-\oint_s W_i\left[\rho\boldsymbol{q}\cdot\boldsymbol{n}-\nu_1\frac{\partial\rho}{\partial n}\right]ds=0 \tag{4a}$$

$$\iint_A\left[\left(\frac{\gamma+1}{2\gamma}\rho u^2-\frac{\gamma-1}{2\gamma}\rho v^2+\frac{\gamma-1}{\gamma}\rho H_\infty\right)\frac{\partial W_i}{\partial x}+\rho u v\frac{\partial W_i}{\partial y}\right]dA-\iint_A\nu_2\left(\frac{\partial u}{\partial x}\frac{\partial W_i}{\partial x}+\frac{\partial u}{\partial y}\frac{\partial W_i}{\partial y}\right)ds$$
$$-\oint_s W_i\left[\rho u\boldsymbol{q}\cdot\boldsymbol{n}-\nu_2\frac{\partial u}{\partial n}\right]ds-\oint_s W_i p\frac{\partial y}{\partial s}ds=0 \tag{4b}$$

$$\iint_A\left[\rho u v\frac{\partial W_i}{\partial x}+\left(\frac{\gamma+1}{2\gamma}\rho v^2-\frac{\gamma-1}{2\gamma}\rho u^2+\frac{\gamma-1}{\gamma}\rho H_\infty\right)\times\frac{\partial W_i}{\partial y}\right]dA-\iint_A\nu_2\left(\frac{\partial v}{\partial x}\frac{\partial W_i}{\partial x}+\frac{\partial v}{\partial y}\frac{\partial W_i}{\partial y}\right)dA$$
$$-\oint_s W_i\left[\rho v\boldsymbol{q}\cdot\boldsymbol{n}-\nu_2\frac{\partial v}{\partial n}\right]ds+\oint_s W_i p\frac{\partial x}{\partial s}ds=0 \tag{4c}$$

$$\boldsymbol{q}=u\boldsymbol{i}+v\boldsymbol{j}$$

The integration by parts results in contour integrals that are assumed, in the weak form, to cancel each other on element edges in the interior of the domain with the result that the formulation remains fully conservative with respect to fluxes.

It should also be remarked that, while the pressure has been eliminated as a variable in the field, it is left in the contour integrals because it may be a given quantity along some segments of these contours. In addition, while ρ, u, and v are used as the solution variables, nothing precludes the selection of the conservative variables ρ, ρu, and ρv as the solution variables, at the expense, however, of added complexity in the formation of the Jacobian of the Newton method.

Newton Linearization

Newton's linearization is introduced by setting

$$U^{n+1}=U^n+\Delta U$$

Upon substituting and neglecting second-order terms (e.g., $\Delta u\,\Delta\rho$), Eqs. (4) can be recast in Δ form. For the continuity equation one obtains

$$\iint_A\left[\left(u\frac{\partial W_i}{\partial x}+v\frac{\partial W_i}{\partial y}\right)^n\Delta\rho-\nu_1\left(\frac{\partial\Delta\rho}{\partial x}\frac{\partial W_i}{\partial x}+\frac{\partial\Delta\rho}{\partial y}\frac{\partial W_i}{\partial y}\right)\right]dA$$
$$+\iint_A\rho^n\left(\frac{\partial W_i}{\partial x}\Delta u+\frac{\partial W_i}{\partial y}\Delta v\right)dA$$
$$=\oint_s W_i\left[(\rho\boldsymbol{q}\cdot\boldsymbol{n})-\nu_1\frac{\partial\rho}{\partial n}\right]ds-\iint_A\left[\rho u\frac{\partial W_i}{\partial x}+\rho v\frac{\partial W_i}{\partial y}\right.$$
$$\left.-\nu_1\left(\frac{\partial\rho}{\partial x}\frac{\partial W_i}{\partial x}+\frac{\partial\rho}{\partial y}\frac{\partial W_i}{\partial y}\right)\right]^n dA \tag{5a}$$

While for the x-momentum equation

$$\iint_A \left[\left(\frac{\gamma+1}{2\gamma} u^2 - \frac{\gamma-1}{2\gamma} v^2 + \frac{\gamma-1}{\gamma} H_\infty \right) \frac{\partial W_i}{\partial x} + uv \frac{\partial W_i}{\partial y} \right]^n \Delta\rho \, dA + \iint_A \left[\left(\frac{\gamma+1}{\gamma} \rho u \frac{\partial W_i}{\partial x} + \rho v \frac{\partial W_i}{\partial y} \right)^n \Delta u - \nu_2 \left(\frac{\partial \Delta u}{\partial x} \frac{\partial W_i}{\partial x} + \frac{\partial \Delta u}{\partial y} \frac{\partial W_i}{\partial y} \right) \right] dA + \iint_A \left(\frac{\gamma-1}{\gamma} \rho v \frac{\partial W_i}{\partial x} - \rho u \frac{\partial W_i}{\partial y} \right)^n \Delta v \, dA = \oint_s W_i \left[(\rho u q \cdot n) - \nu_2 \frac{\partial u}{\partial n} \right] ds + \oint_s W_i p \frac{\partial y}{\partial s} ds + \nu_2 \iint_A \left(\frac{\partial u}{\partial x} \frac{\partial W_i}{\partial x} + \frac{\partial u}{\partial y} \frac{\partial W_i}{\partial y} \right)^n dA - \iint_A \left[\left(\frac{\gamma+1}{2\gamma} \rho u^2 - \frac{\gamma-1}{2\gamma} \rho v^2 + \frac{\gamma-1}{\gamma} \rho H_\infty \right) \frac{\partial W_i}{\partial x} + \rho u v \frac{\partial W_i}{\partial y} \right]^n dA \tag{5b}$$

The form of the y-momentum equation is similar.

Finite Element Discretization

The final step consists of the introduction of the finite element interpolation polynomials. The spatial discretization is based on quadrilateral bilinear elements where, in each element, the variables vector U is expressed as a bilinear function of the cell vertex values, $(\hat{U})$:

$$U = \sum_{j=1}^{4} N_j(\xi,\eta) \hat{U}_j \tag{6}$$

$$N_j(\xi,\eta) = \tfrac{1}{4}(1+\xi\xi_j)(1+\eta\eta_j) \qquad j = 1, \ldots, 4$$

Substituting Eq. (6) into Eqs. (5), and summing over the elements yields, at a node i

$$\sum_{e=1}^{E} \left[\sum_{j=1}^{4} \left\{ \left[k^\rho_{i,j}\right]_\rho \Delta\hat{\rho}_j + \left[k^u_{i,j}\right]_\rho \Delta\hat{u}_j + \left[k^v_{i,j}\right]_\rho \Delta\hat{v}_j \right\} \right] = -(R_i)_\rho \tag{7a}$$

$$\sum_{e=1}^{E} \left[\sum_{j=1}^{4} \left\{ \left[k^\rho_{i,j}\right]_u \Delta\hat{\rho}_j + \left[k^u_{i,j}\right]_u \Delta\hat{u}_j + \left[k^v_{i,j}\right]_u \Delta\hat{v}_j \right\} \right] = -(R_i)_u \tag{7b}$$

$$\sum_{e=1}^{E} \left[\sum_{j=1}^{4} \left\{ \left[k^\rho_{i,j}\right]_v \Delta\hat{\rho}_j + \left[k^u_{i,j}\right]_v \Delta\hat{u}_j + \left[k^v_{i,j}\right]_v \Delta\hat{v}_j \right\} \right] = -(R_i)_v \tag{7c}$$

where the $[k_{i,j}]$ are element influence matrices and (R_i) indicate the residuals of Eqs. (4) at node i.

For the continuity equation the coefficients explicitly are

$$\left[k^\rho_{i,j}\right]_\rho = \iint_A N_j \left(u \frac{\partial W_i}{\partial x} + v \frac{\partial W_i}{\partial y} \right)^n dA - \nu_1 \iint_A \left(\frac{\partial W_i}{\partial x} \frac{\partial N_j}{\partial x} + \frac{\partial W_i}{\partial y} \frac{\partial N_j}{\partial y} \right) dA$$

$$\left[k^u_{i,j}\right]_\rho = \iint_A \rho^n N_j \frac{\partial W_i}{\partial x} dA$$

$$\left[k^v_{i,j}\right]_\rho = \iint_A \rho^n N_j \frac{\partial W_i}{\partial y} dA$$

For the x-momentum equation the coefficients are

$$\left[k^\rho_{i,j}\right]_u = \iint_A \left[\left(\frac{\gamma+1}{2\gamma} u^2 - \frac{\gamma-1}{2\gamma} v^2 + \frac{\gamma-1}{\gamma} H_\infty \right) \frac{\partial W_i}{\partial x} + uv \frac{\partial W_i}{\partial y} \right]^n N_j \, dA$$

$$\left[k^u_{i,j}\right]_u = \iint_A \left[N_j \left(\frac{\gamma+1}{\gamma} \rho u \frac{\partial W_i}{\partial x} + \rho v \frac{\partial W_i}{\partial y} \right) - \nu_2 \left(\frac{\partial W_i}{\partial x} \frac{\partial N_j}{\partial x} + \frac{\partial W_i}{\partial y} \frac{\partial N_j}{\partial y} \right) \right]^n dA$$

$$\left[k^v_{i,j}\right]_u = \iint_A N_j \left(\frac{\gamma-1}{\gamma} \rho v \frac{\partial W_i}{\partial x} - \rho u \frac{\partial W_i}{\partial y} \right)^n dA$$

The form of the y-momentum equation is similar.

All area integrals are numerically evaluated by a Gaussian quadrature procedure, using a (3×3) grid of sampling points.

The elements influence matrices are assembled into a global matrix and the system of algebraic equations is in the form

$$[K]^n \Delta U = -R^n \tag{8}$$

where ΔU is the vector of unknowns $\Delta\rho$, Δu, Δv. Convergence of this nonlinear process can therefore be measured directly from the right-hand side, i.e., the residual, by a norm. Here the L_2 norm is used and defined as

$$|L|_2 = \left\{ \frac{1}{\mathrm{DOF}} \sum_{i=1}^{\mathrm{DOF}} (R_i^n)^2 \right\}^{1/2}$$

where DOF is the total number of cell-vertex unknowns or degrees of freedom.

III. Boundary Conditions

At inflow boundaries all three variables, ρ, u, v, must be specified. At subsonic outflow boundaries the pressure is specified and is accounted for through the pressure contour integrals in the momentum equations.

The boundary conditions at solid boundaries merit some discussion. Three types of contour integrals appear in the discretization of the governing equations: flux, pressure, and artificial viscosity. In finite difference calculations[13] one can use the fact that vorticity is constant along a streamline to calculate the boundary condition for the artificial viscosity term. In finite volumes,[15] the contribution of the normal component of the viscous term is usually neglected in the volumes adjacent to the walls. In the present finite element approach, the only boundary condition imposed directly on the calculation is the no-penetration through solid boundaries, this being done by neglecting the line integral of mass flux in the continuity equation, at walls. All other contour integrals are evaluated using the finite element interpolation and the nodal values. We found that this is the best strategy to minimize the effect of the artificial viscosity on the calculations. The results demonstrate that the numerical momentum flux through the solid boundary is almost machine zero, except at the stagnation points, where it is two orders of magnitude higher than the truncation error.

IV. Solution Procedure

The simple type of artificial viscosity selected provides a continuation mechanism for the Newton method when it is started with a poor initial guess, here taken as uniform flow. First, the artificial viscosity coefficient μ, is set to a high value and the iterative procedure is carried out until the norm of each residual drops below an intermediate limit, say 10^{-5}. At that point, the artificial viscosity coefficient is reduced and the iteration is resumed with the previous converged results as the new initial guess. The cycling of the artificial viscosity coefficient is continued until it reaches the lowest possible value.

Normally only three cycles are required and overall convergence to machine accuracy can be obtained in a total of 15 to 17 iterations. This technique produces faster global convergence than the more conventional approach of adding time-dependent terms to under-relax the solution until the residual begins to decrease.[14]

The Newton-Galerkin formulation leads to a system of banded, sparse, coupled linear algebraic equations, which may not always be well conditioned. A Gauss elimination solver is therefore preferable. Three approaches have been taken to solve the system: a banded Gauss solver, a Frontal solver, and a sparse matrix solver.

In a Gauss elimination banded scheme, the storage and CPU solution times are not excessive for medium-sized two-dimensional grids. The solver can also be easily parallelized through the inner or middle loop of the matrix factorization algorithm. On a Silicon Graphics IRIS4D-240, it was found that the reduced inter-process communication associated with the parallelization of the middle loop, however, yielded a better performance and a speedup of 3.25 in factorization time with four processors was achieved compared to a single processor.

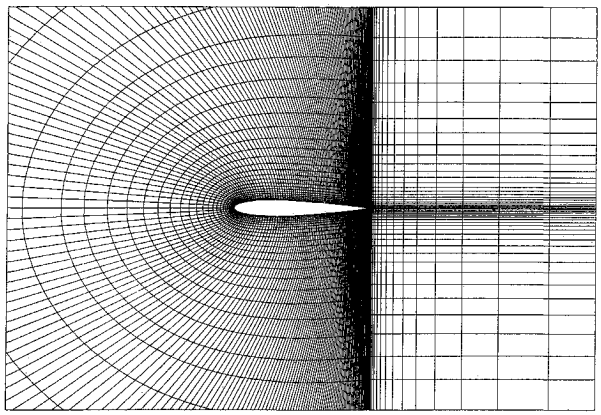

Fig. 1 Finite element C-grid around NACA0012 airfoil, (254×30) with 204 nodes on body.

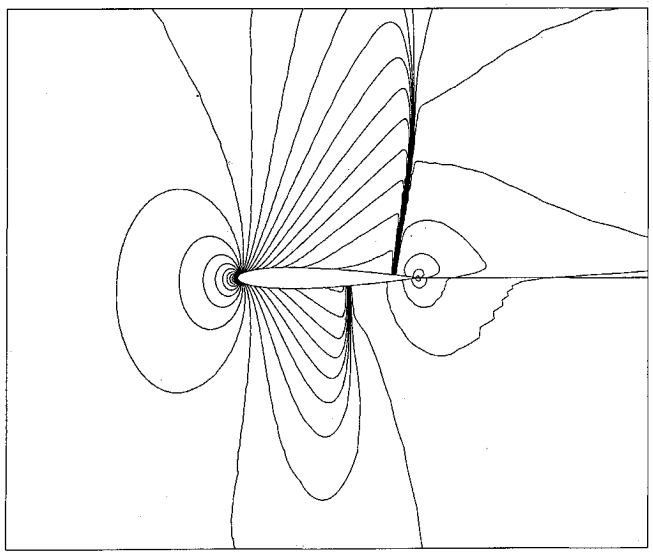

a) Mach number contours around NACA0012 airfoil

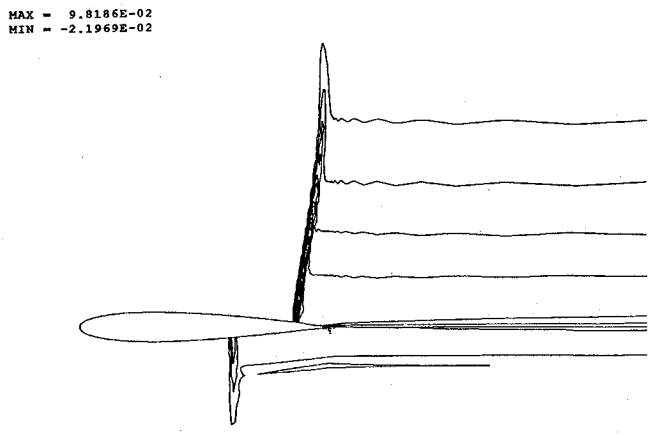

b) Total pressure contours around NACA0012 airfoil

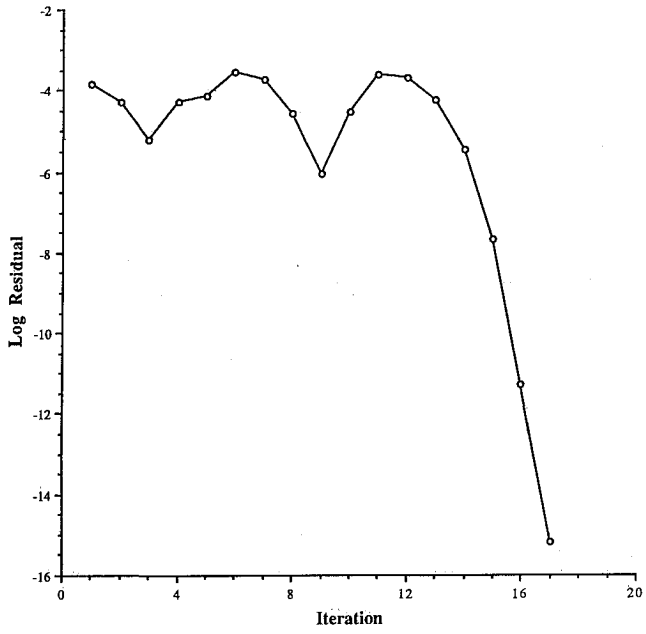

c) Newton iteration convergence history for NACA0012 airfoil, with three cycles of artificial viscosity, $\mu = 5.0$, 0.75 and 0.25

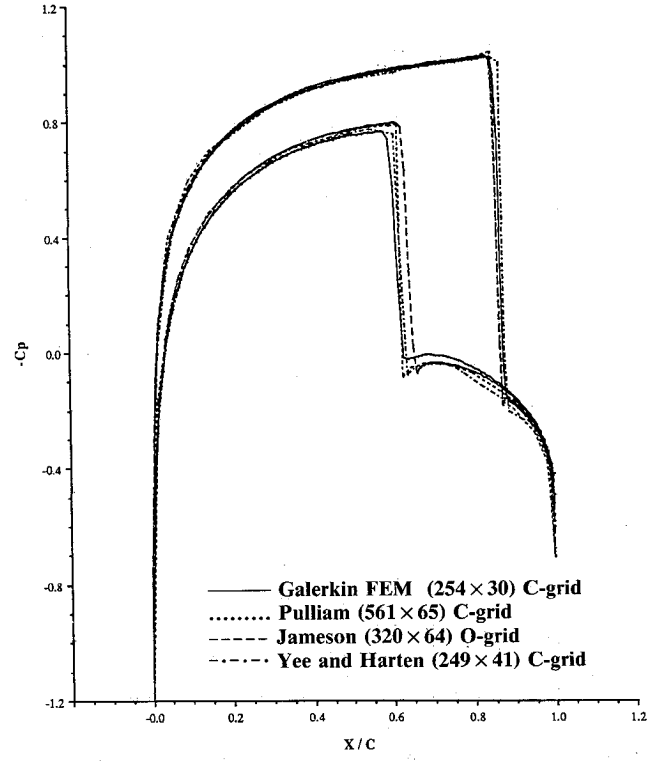

d) C_p distribution around NACA0012 airfoil and comparison to other methods

Fig. 2 Solution for AGARD02 test case.

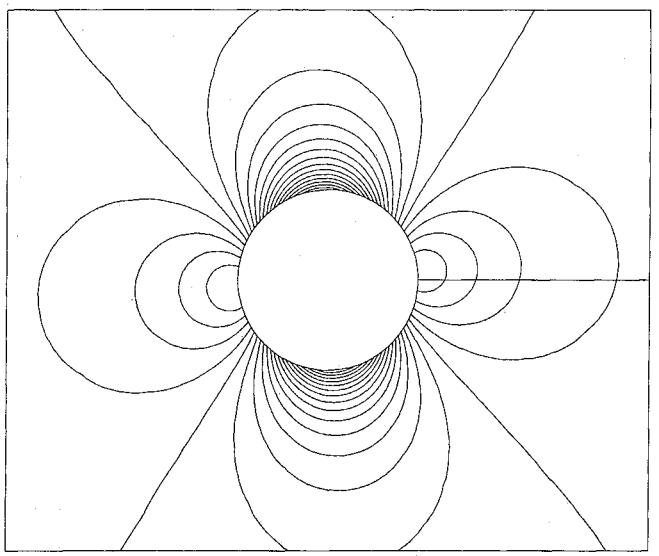

a) Static pressure contours around circular cylinder

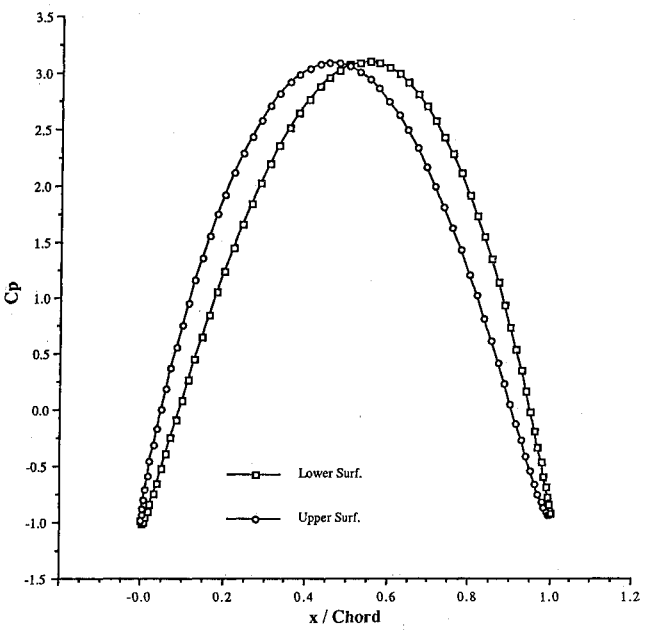

b) C_p distribution around circular cylinder

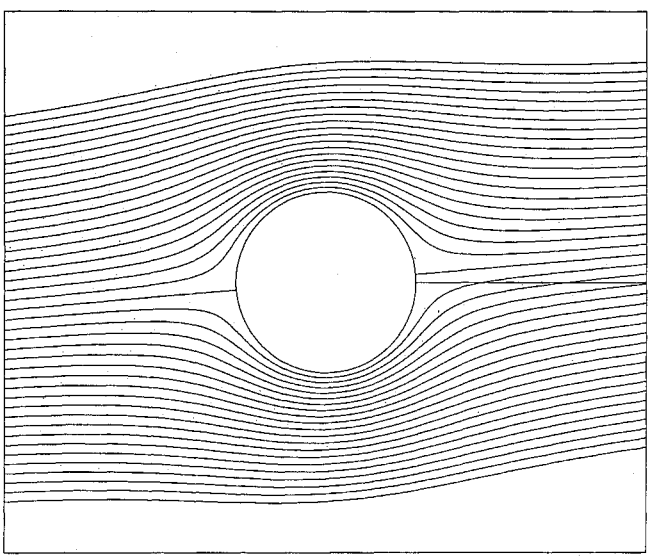

c) Streamline pattern around circular cylinder

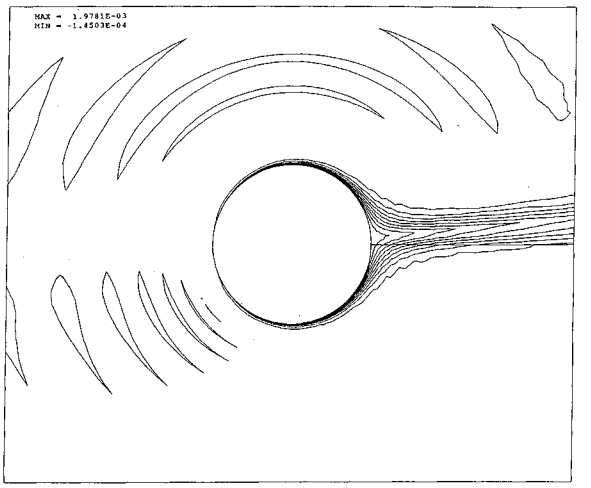

d) Total pressure contours around circular cylinder

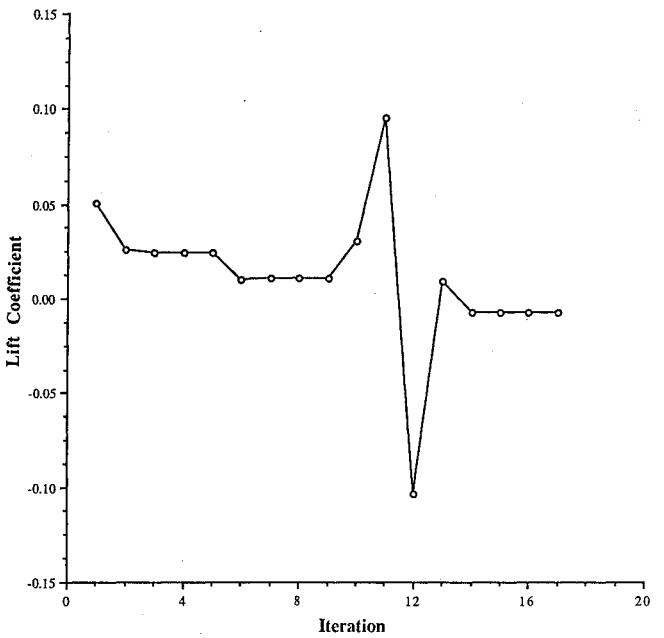

e) History of C_L for flow around circular cylinder

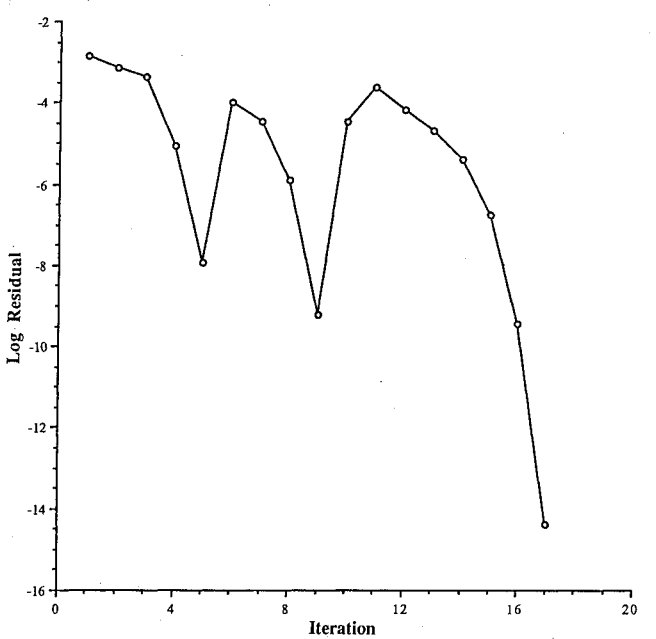

f) Newton iteration convergence history for circular cylinder, with 3 cycles of artificial viscosity, $\mu = 1.0, 0.3, 0.1$

Fig. 3 Solution for the circular cylinder test case, (128×48) O-grid.

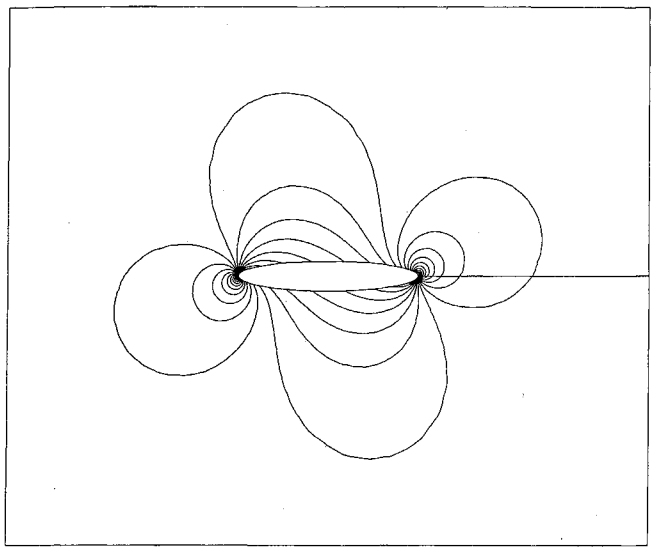

a) Static pressure contours around ellipse

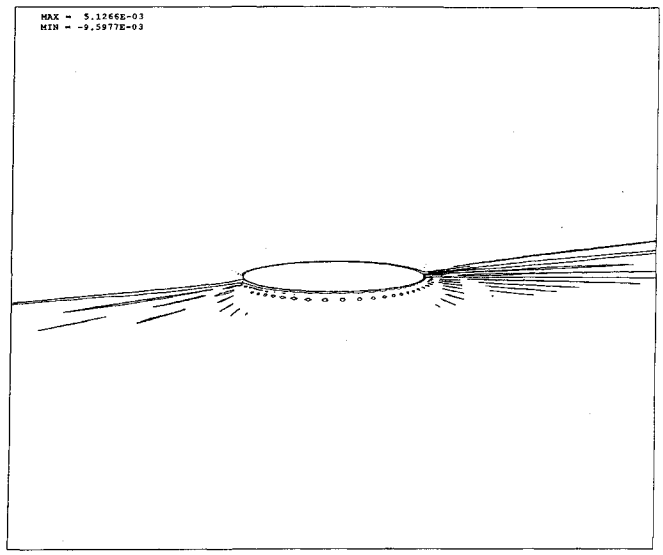

d) Total pressure contours around ellipse

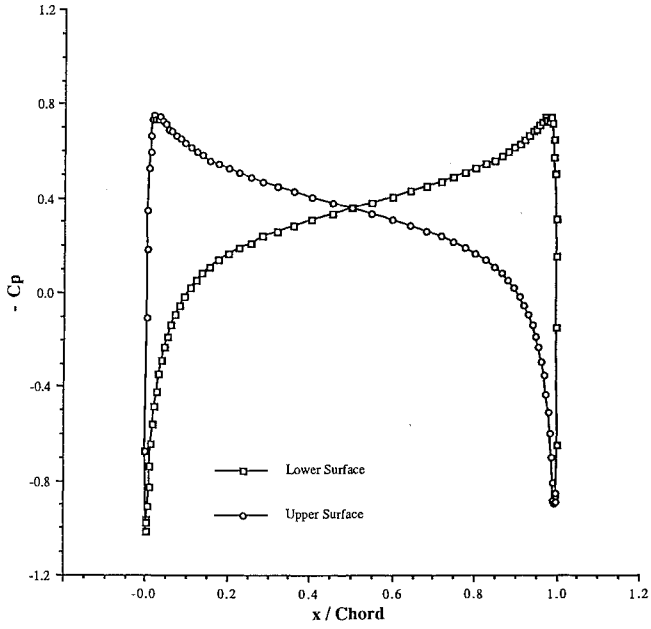

b) C_p distribution around ellipse

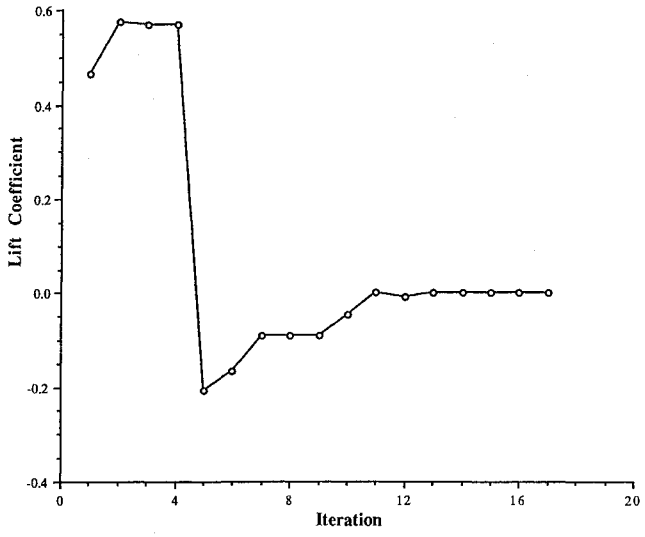

e) History of C_L for flow around ellipse

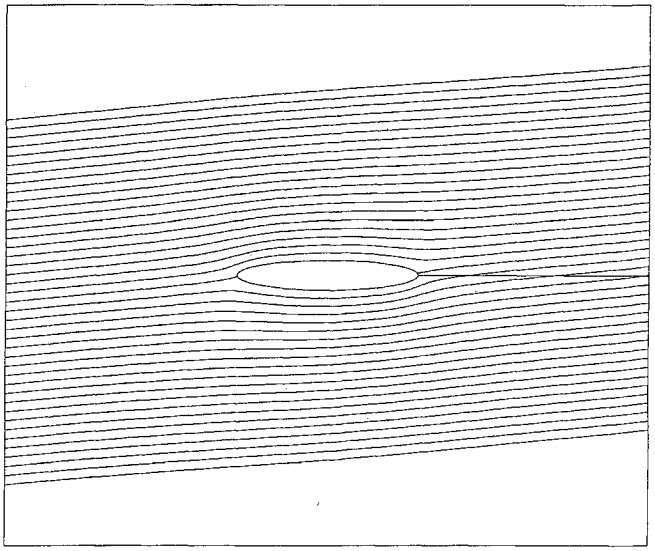

c) Streamline pattern around ellipse

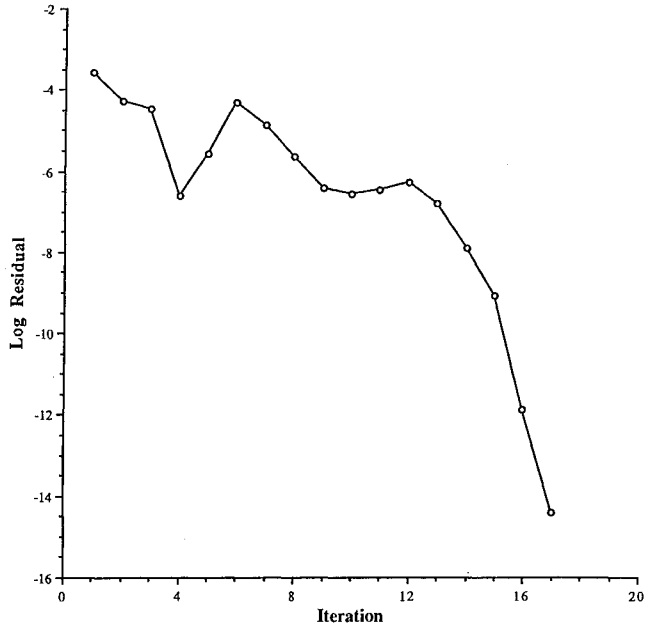

f) Newton iteration convergence history for ellipse, with four cycles of artificial viscosity, $\mu = 0.025$, 0.0025, 0.0015 and 0.001

Fig. 4 Solution for the ellipse test case, (128 × 48) O-grid.

A sparse matrix solver, SPARSPAK, has also been used. Two reordering techniques, the nested dissection and multiple minimum degree algorithms, have been tested and the results indicate the latter to be marginally superior. The multiple minimum degree algorithm yielded a factor of up to 2.84 reduction in storage and a factor of 2.12 reduction in factorization time against the banded solver for the test cases attempted.

For the circular cylinder and ellipse cases presented below, the banded solver required 11.54 MWords of storage for a matrix size of 18,621 degrees of freedom with a bandwidth of 600. The matrix size for the airfoil problem was 22,872 degrees of freedom with a bandwidth of 371. For such two-dimensional problems, SPARSPAK required one third of the storage and halved the solution time per iteration. No effort, however, has been made to parallelize the sparse matrix package.

V. Results

The results are aimed at validating the method for transonic test cases over airfoils and subsonic test cases over bodies such as cylinders and ellipses. All test cases have been converged to machine accuracy and demonstrate quadratic convergence of the Newton algorithm.

AGARD02 Transonic Test Case

The airfoil analyzed is the AGARD02 case[15] for a NACA-0012 airfoil in transonic flow. Figure 1 shows the finite element C-grid (254×30) around the airfoil, extending to 30 chords in the farfield and 25 chords in the wake region. The airfoil is defined by 204 nodes and a total of 7620 elements are used. Figures 2a and 2b display the Mach number and total pressure contours for the flow at a freestream Mach number of 0.85 and an angle of attack of 1 deg. Figure 2c shows the convergence of the iteration scheme for this test case, which includes three cycles of the artificial viscosity coefficient, $\mu = 5.0$, 0.75 and 0.25, and as can be seen, is quadratic for each cycle.

The C_p distribution is compared in Fig. 2d to the results of Jameson,[15] Pulliam,[16] and Yee and Harten,[17] showing good agreement with the three approaches, all using finer grids. For example Pulliam results are for a (561×65) C-grid, Jameson's for a (320×64) O-grid and Yee and Harten's for a (249×41) C-grid. The lift coefficient, $C_L = 0.3926$, compares well to the value of 0.3938 obtained by Pulliam.

Circular Cylinder and Ellipse

Several well-established Euler codes use a number of user-adjustable parameters to introduce numerical dissipation for stability and complex schemes to implement the boundary conditions. Often, some inaccuracies of these methods are masked by the complexity of the flows analyzed. In a recent paper, Pulliam[18] made an exhaustive review of several Euler schemes applied to "simple," if not the simplest, geometries such as circular cylinders and ellipses under nonlifting subsonic conditions. The surprising conclusion was that all codes, for at least one of these two geometries, would predict large values of lift if the freestream is not aligned with a grid line. Similar problems had also been detected by Von Lavante and Melson[19] who calculated the flow over a 2:1 and a 6:1 ellipse at a Mach number of 0.4 and 3 degrees angle of attack and came to such a puzzling conclusion. Pulliam challenged the CFD community to demonstrate or develop schemes that do not suffer from such inaccuracies. The present finite element algorithm has been tested for the specific test cases and grid density suggested in the Pulliam paper and has been verified for consistency of results.

First, flow over a circular cylinder at a Mach number of 0.2 and an angle of attack of 5 deg is computed. The grid, skewed to the direction of the freestream, has (128×48) grid points and 6144 quadrilateral bilinear elements. The farfield boundary is set at 45 diameters with no farfield vortex correction. The results obtained are shown in Figs. 3 and the static pressure contours on the upper and lower surfaces, Fig. 3a, can be seen to be virtual mirror images of each other with respect to the axis formed by the freestream, yielding a C_L of 6.887×10^{-3}. This compares to a value of 13.66 in the Pulliam paper. Figure 3b shows the C_P distribution over the cylinder, again demonstrating the antisymmetry of the pressure distribution at the surface. The solution also yields stagnation points aligned with the flow, as shown in Fig. 3c. While the artificial viscosity effects are demonstrated to be minimal, it is clear from the total pressure contours of Fig. 3d that it still causes a wake behind the cylinder, carried to the outer boundary.

The C_L history during the iterative process is shown in Fig. 3e and can be seen to cross the zero lift condition during convergence. Hence, to avoid any ambiguities in interpreting the quality of the results, the Newton iteration is carried to machine accuracy, as shown in Fig. 3f.

Second, the flow over a 6:1 ellipse at a freestream Mach number of 0.2 and an angle of attack of 5 deg is computed. This is the more demanding of the two test cases, according to Pulliam. The grid, skewed to the direction of the freestream, has the same density as the circular cylinder case and the same farfield distance. The results obtained are shown in Figs. 4. The static pressure contours, Fig. 4a, are virtually reverse mirror images of each other with respect to the axis formed by the freestream direction, yielding a C_L of 1.215×10^{-3}. This, for example, compares to a value of 1.545 for ARC2D.[18] Figure 4b shows the nearly antisymmetric C_P distribution over the ellipse and the stagnation points can be seen from Fig. 4c to be aligned with the flow. The effect of the artificial viscosity is shown in the total pressure contours of Fig. 4d.

Figure 4e shows the C_L history, which similar to the circular cylinder case, crosses the zero lift value during convergence. The quadratic convergence of the Newton iteration, to machine accuracy, is demonstrated in Fig. 4f.

Other test cases have been carried out to verify the consistency of the ellipse results and their independence from angle of attack and Mach number. A test has been run on the same grid, at a Mach number of 0.4 and an angle of attack of 3 deg corresponding to the flow conditions of Von Lavante and Melson.[19] The obtained value for C_L was 2.791×10^{-2} and demonstrates that the results are nearly independent of Mach number and angle of attack.

Solution times for the airfoil are of the order of 20 s/iteration on a Cray X-MP and of the order of 27 s/iteration for the circular cylinder and ellipse cases.

VI. Conclusion

A finite element method for the solution of the Euler equations in primitive variable form has been developed, with artificial viscosity introduced in the simple form of Laplacians added to the governing equations. A weak-Galerkin formulation permits a compact and accurate treatment of boundary conditions that otherwise require extrapolation. A simple continuation mechanism is introduced through the variation of a single viscosity parameter.

A Newton linearization method and a fully coupled direct solver have been used to solve the nonlinear system. Convergence of the iterative method is demonstrated to be quadratic, taking very few iterations to reach machine accuracy.

For large-scale problems, work is focusing on new concepts in direct solver technology and iterative approaches such as preconditioned conjugate gradient methods to reduce storage and solution times.

In addition, work is progressing on increasing the accuracy of the scheme to second order. Nevertheless, at the present time, this simple, straightforward, constant, first-order scheme has succeeded in responding to the challenge presented to the CFD community by Pulliam at the 1989 AIAA Reno Conference.

Acknowledgments

This work was supported under Operating Grant OGPIN013 and Strategic Grant STREQ040 of the Natural Sciences and Engineering Research Council of Canada (NSERC).

References

[1]Fletcher, C. A. J., "A Primitive Variable Finite Element Formulation for Inviscid Compressible Flow," *Journal of Computational Physics*, Vol. 33, 1979, pp. 301-312.

[2]Tezduyar, T. E., and Hughes, T. J. R., "Finite Element Formulations for Convection Dominated Flows with Particular Emphasis on the Compressible Euler Equations," AIAA Paper 83-0125, 1983.

[3]Angrand, F., Dervieux, A., Boulard, V., Périaux, J., and Vijayasundaran, G., "Transonic Euler Simulations by Means of Finite Element Explicit Schemes," AIAA Paper 83-1924, 1983.

[4]Stoufflet, B., "Implicit Finite Element Methods for the Euler Equations," *Numerical Methods for the Euler Equations of Fluid Dynamics*, edited by F. Angrand, et al., SIAM, Philadelphia, PA, 1985, pp. 409-434.

[5]Donea, J., "A Taylor-Galerkin Method for Convective Transport Problems," *International Journal for Numerical Methods in Engineering*, Vol. 20, 1984, pp. 101-119.

[6]Löhner, R., Morgan, K., and Zienkiewicz, O. C., "The Solution of Non-Linear Hyperbolic Equation Systems by the Finite Element Method" *International Journal for Numerical Methods in Fluids*, Vol. 4, Nov. 1984, pp. 1043-1063.

[7]Peraire, J., Peiro, J., Formaggia, L., Morgan, K., and Zienkiewicz, O. C., "Finite Element Euler Computations in Three Dimensions," *Proceedings of the International Conference on Computational Methods in Flow Analysis*, Okayama, Sept. 1988, pp. 3-25.

[8]Bruneau, C. H., Laminie, J., and Chattôt, J. J., "Computation of 3-D Vortex Flows Past a Flat Plate at Incidence Through a Variational Approach of the Full Steady Euler Equations," *International Journal for Numerical Methods in Fluids*, Vol. 9, March 1989, pp. 305-323.

[9]Hafez, M., Palaniswamy, S., and Mariani, P., "Calculation of Transonic Flows with Shocks Using Newton's Method and Direct Solver, Part II," AIAA Paper 88-0226, Jan. 1988.

[10]Baruzzi, G. S., "Finite Element Solutions of the Euler Equations in Primitive Variables Form," M. Eng. Thesis, Dept. of Mechanical Engineering, Concordia Univ., Montreal, Quebec, Canada, 1989.

[11]Roe, P. L., and Van Leer, B., "Non-Existence, Non-Uniqueness and Slow Convergence in Discrete Conservation Laws," *Numerical Methods for Fluid Dynamics*, edited by K. Morton and M. Baines, Clarendon, Oxford, England, UK, 1988.

[12]Baruzzi, G., Habashi, W. G., and Hafez, M. M., "Non-Unique Solutions of the Euler Equations" *Advances in Fluid Dynamics*, edited by W. F. Ballhaus, Jr. and M. Y. Hussaini, Springer-Verlag, New York, 1989, pp. 1-10.

[13]Hafez, M. M., Yam, C., Tang, K., and Dwyer, H., "Calculations of Rotational Flows Using Stream Function," AIAA Paper 89-0474, Jan. 1989.

[14]Venkatakrishnan, V., "Newton Solution of Inviscid and Viscous Problems," *AIAA Journal*, Vol. 27, No. 7, 1989, pp. 885-891.

[15]AGARD Working Group 07, "Test Cases for Inviscid Flow Field Methods," AGARD-AR-211, 1985.

[16]Pulliam, T. H., and Barton, T. J., "Euler Computations of AGARD Group 07 Airfoil Test Cases," AIAA Paper 85-0018, Jan. 1985.

[17]Yee, H. C., and Harten, A., "Implicit TVD Schemes for Hyperbolic Conservation Laws in Curvilinear Coordinates," *AIAA Journal*, Vol. 25, No. 2, 1987, pp. 266-274.

[18]Pulliam, T. H., "A Computational Challenge: Euler Solutions for Ellipses," AIAA Paper 89-0469, Jan. 1989.

[19]Von Lavante, E., and Melson, N. D., "Simple Numerical Method for Solving the Steady Euler Equations," *Numerical Methods in Laminar and Turbulent Flow*, edited by C. Taylor, W. G. Habashi, and M. M. Hafez, Pineridge Press, Swansea, Wales, UK, 1987, pp. 2051-2062.